IEEE Photonics Journal
An IEEE Photonics Society Publication

Open Access

A Phase Distribution Design Method for Phased Arrays Multibeam Independently Generating and 3-D Scanning

Volume 6, Number 5, October 2014

Dong Wang
Yu-Li Wu
Bao-Quan Jin
Peng Jia
Dong-Mei Cai

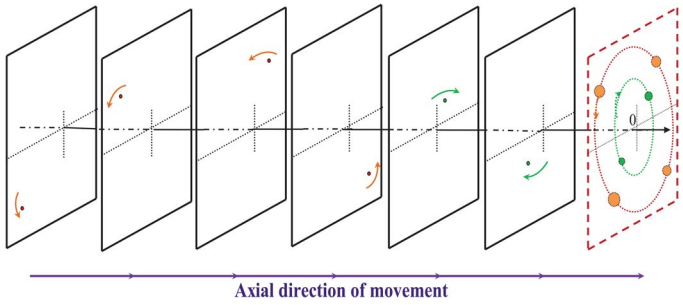

DOI: 10.1109/JPHOT.2014.2345882
1943-0655

IEEE photonics SOCIETY

IEEE

A Phase Distribution Design Method for Phased Arrays Multibeam Independently Generating and 3-D Scanning

Dong Wang,[1,2] Yu-Li Wu,[1] Bao-Quan Jin,[1] Peng Jia,[1] and Dong-Mei Cai[1]

[1]Key Laboratory of Advanced Transducers and Intelligent Control System, Ministry of Education, and Shanxi Province, College of Physics and Optoelectronics, Taiyuan University of Technology, Taiyuan 030024, China
[2]Institute of Ultra-Precision Optoelectronic Instrument Engineering, Harbin Institute of Technology, Harbin 150080, China

DOI: 10.1109/JPHOT.2014.2345882

Manuscript received June 22, 2014; revised July 30, 2014; accepted July 30, 2014. Date of publication August 6, 2014; date of current version August 25, 2014. This work was supported in part by the Shanxi Natural Science Foundation under Grant 2013011006-4 and in part by the Qualified Personnel Foundation of Taiyuan University of Technology under Grant tyutrc-2013. Corresponding author: D. Wang (e-mail: wangdongwind@gmail.com).

Abstract: This paper reports the realization of a phase distribution design method for phased arrays multibeam independently generating and 3-D scanning. The phase distribution design method inherits the projection optimization idea from the generalized adaptive-additive algorithm; however, a striking difference here is that the iteration plane is not just one but multiple, which means the method promises to be not only suitable for creating phase distributions for multibeam independently lateral scanning but capable of creating phase distributions for independently axial scanning as well. Both simulations and experiments were conducted to investigate the performance of the method; simulation agrees with experimental results, which validates the effectiveness of the method proposed. The technique described in this paper could provide a promising convenient multibeam generating and 3-D scanning for ladar, laser weapons, laser micromachining, etc.

Index Terms: Diffractive optics, phased arrays, multi-beam, 3-D scanning.

1. Introduction

Phased arrays can be considered as a pure phase-type diffraction element, which consists of a large number of phase-delay-programmable units [1]–[4]. Phase delay of each unit forms a phase distribution, the phase distribution can be naturally coded as expected [5]. Then, the splitting and scanning of light beam exiting the phased arrays can be achieved by appropriately coding the phase distribution, i.e., phased array multi-beam scanning technology (PAMST).

PAMST is an important approach to achieve ladar [6], [7], laser weapons [8], laser micromachining [9], [10] and other optical systems [20]–[24], and the core issue of PAMST is how to design the phase distribution of phased arrays. So far, most of the existing phase distribution design methods have been only applicable to multi-beam two-dimensional scanning (M2-DS), and the typical ones of these methods are the blazed grating (BG) [3], [11]–[13], Yang-Gu (YG) [14], [15], Gerchburg-Saxton (GS) [16], [17] and Generalized Adaptive-Additive (GAA) [18], [19] method. On the phase distribution design methods for multi-beam 3-D scanning

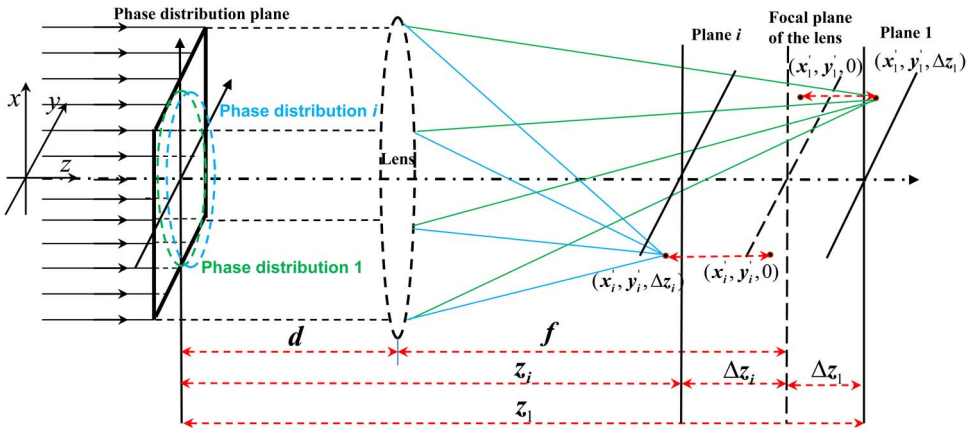

Fig. 1. Schematic of the multiplane GAA method for controlling multiple focal spots.

(M3-DS), there have been just several reports [20]–[24]. By adding a lens term to the BGs, Liesener *et al.* proposed an improved BG method for the 3-D scanning of multi-optical tweezers [20]. For reconstructing 3-D objects, Haist *et al.*, presented an improved version of GS method [21], which was called as the multiplane GS algorithm by Sinclair *et al.* and used for the 3-D scanning of multi-optical tweezers [22]. In order for 3-D beam shaping, Shabtay reported an improved version of GS method involved Ewald's surfaces [23], which was demonstrated experimentally and called as the 3-D GS algorithm by Whyte *et al.* [24]. And among the typical methods for M2-DS above-mentioned, the most frequently used methods are the GS and GAA method and the GAA method is one of the improved versions of the GS method. Ever since Curtis et al. firstly applied the GAA method for M2-DS of dynamic holographic optical tweezers [18], it has been gradually well known and become a popular way for the M2-DS. Recently, for M2-DS applications, the GAA method had been proven to be better than GS method on the uniformity of the beam, while the efficiency of the light beam were almost the same for both of them [25], [26]. However, up to now, there has been no report on the multiplane GAA method for phased array M3-DS.

Since the GAA method is only suitable for creating phase distributions for phased arrays multi-beam independently lateral scanning, therefore, we propose the multiplane GAA method and firstly demonstrate it for phased arrays multi-beam independently generating and 3-D scanning. The multiplane GAA method inherits the projection optimization idea from the GAA method, but, a striking difference here is that the iteration plane is not just one but multiple, which promises the method to be, not only suitable for creating phase distributions for phased arrays multi-beam independently lateral scanning, but also capable of creating phase distributions for the independently axial scanning. The realization of the method proposed here would provide a promising convenient multi-beam generating and 3-D scanning for ladar, laser weapons, laser micromachining, etc.

The paper is organized as follows. In Section II, an overview of the multiplane GAA method is presented. In Section III, simulations and discussions are given. In Section IV, experiments and discussions are given. Finally, a summary is given in Section V.

2. Overview of the Multiplane GAA Method

As shown in Fig. 1, in order to independently move each of the multiple focal spots from the original focal plan of the lens, the multiplane GAA method was improved from the GAA method and the difference between them was that the iteration plane is not just one but multiple, which promises the method to be, not only capable of creating phase distributions for the independently axial scanning, but also suitable for creating phase distributions for phased arrays multi-beam independently lateral scanning. As shown in Fig. 1, there is just one focal spot in each of

the multiple focal planes, using the proposed method the focal spot can be controlled to move laterally in there, and the plane itself can be controlled to move axially, which makes the 3-D scanning of a focal spot possible. Therefore, a corresponding phase distribution (e.g. phase distribution ***i***) is needed to be designed for the controlling of a focal spot (e.g. focal spot ***i***), as shown in Fig. 1.

Using the multiplane GAA method, the design procedures of a phase distribution ***i*** for the controlling of a focal spot ***i*** are as follows:

The amplitude distribution of the light field on the Plane ***i***, where the focal spot ***i*** is (as can be seen in Fig. 1), is assumed as $|D(x_i', y_i')|$, and all the sample values of the amplitude distribution are set as zero except the target focal spot ***i*** with the coordinates (x_i', y_i'). The phase of the light field on the Plane ***i*** is initially given as zero. The phase distribution ***i*** (as can be seen in Fig. 1) can be calculated through the inverse Fourier transform of the light field on the Plane ***i*** by the following four steps. In the ***n***th iteration of the multiplane GAA method, we have the following.

Step 1. The light field $F_n(x_i', y_i')$ on the Plane ***i*** is forced and expressed as

$$F_n(x_i', y_i') = \begin{cases} \beta \cdot \left|D(x_i', y_i')\right| \exp\left[i\varphi'_{n-1}(x_i', y_i')\right], & \text{in target region} \\ F'_{n-1}(x_i', y_i'), & \text{out of target region} \end{cases} \quad (1)$$

where $\beta = [(1-\xi) + \xi|D(x_i', y_i')|/|F_{n-1}(x_i', y_i')|]$, ξ is optimized and chosen as 0.5 for a better uniformity [18], [19]. $F'_{n-1}(x_i', y_i')$ is the output from the Fourier transform of the light field involved the phase distribution ***i*** in the previous iteration and $\varphi'_{n-1}(x_i', y_i')$ is its phase.

Step 2. The light field $T_n^i(x, y)$ involved the phase distribution ***i*** can be obtained through the inverse Fourier transformation of the light field $F_n(x_i', y_i')$ on the Plane ***i***, as follows:

$$T_n^i(x, y) = \int_{-\infty}^{+\infty} \int_{-\infty}^{+\infty} F_n(x_i', y_i') P_i(x, y)^{-1} \exp\left[i2\pi\left(xx_i' + yy_i'\right)\right] dx'dy' = \left|T_n^i(x, y)\right| exp\left[i\varphi_n^i(x, y)\right] \quad (2)$$

where x, y are the coordinates of the light field plane involved the phase distribution ***i*** (called as Phase distribution plane, as shown in Fig. 1). $|T_n^i(x, y)|$ is the amplitude of $T_n^i(x, y)$ and $\varphi_n^i(x, y)$ is the phase of $T_n^i(x, y)$. A phase distribution $P_i(x, y)^{-1}$ of a negative lens was introduced for the Plane ***i*** axially scanning, $P_i(x, y)^{-1} = \exp[j\pi\Delta z_i(x^2 + y^2)/\lambda(d\Delta z_i + f\Delta z_i + f^2)]$ and j is the imaginary unit, λ is the wavelength, d is the distance between the lens plane and the Phase distribution plane (as shown in Fig. 1), f is the focal length of the lens, Δz_i is the distance between the Focal plane of the lens and the Plane ***i***, and Δz_i can take a positive or negative sign which is determined by that the Plane ***i*** is on the left or right of the Focal plane of the lens.

Step 3. By retaining the phase distribution of $T_n^i(x, y)$ and forcing the amplitude distribution to be one, a new light field $H_n^i(x, y)$ in Phase distribution plane for Step 4 is obtained, as follows:

$$H_n^i(x, y) = \begin{cases} \exp\left[i\varphi_n^i(x, y)\right], & \text{in target region} \\ 0, & \text{out of target region.} \end{cases} \quad (3)$$

Step 4. The output light field $F'_n(x_i', y_i')$ on the Plane ***i*** can be calculated by conducting the Fourier transformation of the light field $H_n^i(x, y)$ in Phase distribution plane, as follows:

$$F'_n(x_i', y_i') = \int_{-\infty}^{+\infty} \int_{-\infty}^{+\infty} H_n^i(x, y) P_i(x, y) \exp\left[-i2\pi\left(x_i'x + y_i'y\right)\right] dxdy = |F'_n(x_i', y_i')| \exp\left[i\varphi'_n(x_i', y_i')\right] \quad (4)$$

where $P_i(x, y)$ is a phase distribution of a positive lens which was used to offset the phase distribution $P_i(x, y)^{-1}$ of a negative lens in Step 2.

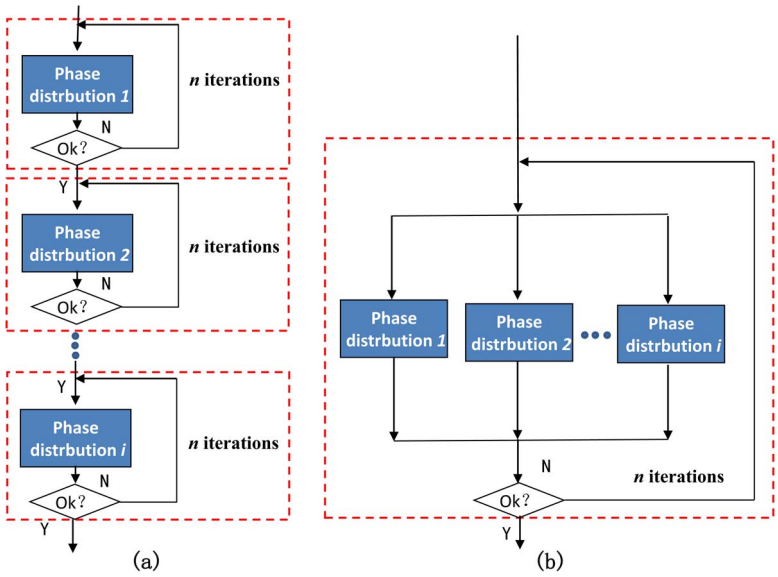

Fig. 2. Two schemes for the multiplane GAA method to design phase distributions for phased arrays M3-DS. (a) Serial iteration version. (b) Parallel iterative version.

After a number of the above 4-Steps iterations, the output amplitude distribution $|F'_n(x'_i, y'_i)|$ will be able to converge to an approximation of the amplitude distribution $|F_n(x'_i, y'_i)|$ of the forced light field $F_n(x'_i, y'_i)$ on the Plane ***i*** in Step 1. Then $\varphi^i_n(x, y)$ is the corresponding phase distribution which can produce this light field on the Plane ***i***.

Obviously, different scanning positions of the focal spot ***i*** need different phase distribution ***i*** $\varphi^i_n(x, y)$, and the control of multiple focal spots scanning needs multiple phase distributions. Then, multiple phase distributions $\varphi^1_n(x, y) + \varphi^2_n(x, y) + \cdots + \varphi^i_n(x, y)$ produce the final phase distribution $\varphi_F(x, y)$ which is to be loaded onto the phased arrays for the desired M3-DS.

As mentioned above, the control of multiple focal spots scanning needs multiple phase distributions. It can be noted that there are two schemes for the multiplane GAA method designing the multiple phase distributions for phased arrays M3-DS. One was called as serial iteration version, in which multiple phase distributions is calculated one by one as shown in Fig. 2(a). Another was called as parallel iterative version, in which multiple phase distributions is calculated simultaneously as shown in Fig. 2(b). It can be predicted that the parallel iterative scheme should be better than the serial iterative scheme, because the serial iterative scheme increases the correlations of the designed phase distributions for phased array M3-DS.

3. Simulations and Discussions

In this Section, simulations were conducted to theoretically investigate the prediction and the above multiplane GAA method for phased arrays M3-DS. Considering the structural parameters of the phased arrays which will be used for the experimental demonstrations in next section, the simulation parameters for the multiplane GAA method were carefully chosen as follows: The wavelength $\lambda = 632.8$ nm, $d = f = 150$ mm, the iteration number $n = 80$, the effective phase distribution diameter was assumed as 7.68 mm and discretized on a grid of 256 $\times$ 256, the phase value on each grid was discretized in 256 levels, and the light field distribution was padded with zero intensity points in each iteration of the multiplane GAA method to create a 512 $\times$ 512 pixel matrix.

First of all, simulations were given to validate the prediction that the parallel iterative scheme shown in Fig. 2(a) was better than the serial iterative scheme shown in Fig. 2(b). Fig. 3 gives the results of the two schemes for generating three focal spots on the same focal planes [as shown

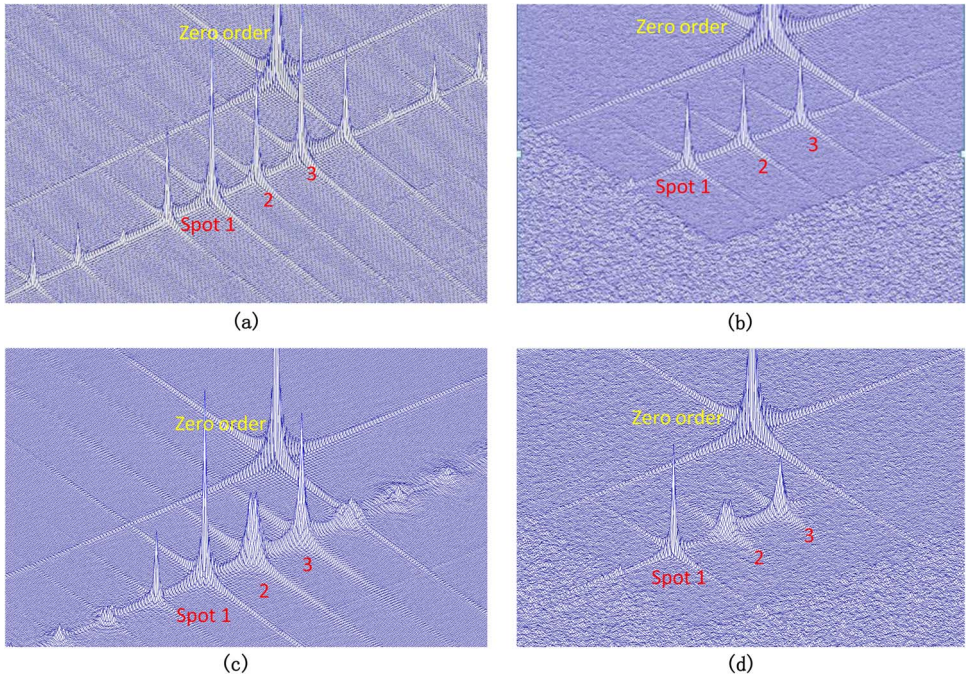

Fig. 3. Simulations of the diffraction of the phase distribution designed by using (a) and (c) the serial iterative version or (b) and (d) the parallel iterative version of the multiplane GAA method for (a) and (b) generating three focal spots on the same focal planes or (c) and (d) generating three focal spots on different focal planes.

in Fig. 3(a) and (b)] or on different focal planes [as shown in Fig. 3(c) and (d)]. Fig. 3(b) and (d) depict the result of the parallel iterative scheme, in which the three focal spots generated using the parallel iterative scheme nearly have no side lobes. Fig. 3(a) and (c) depict the result of the serial iterative scheme, and as can be seen from it the three focal spots generated using the serial iterative scheme have many side lobes, which is believed to be caused by the increased correlations of the phase distributions designed using the serial iterative scheme. Comparing Fig. 3 (b) and (d) with Fig. 3(a) and (c) apparently shows that the parallel iterative scheme is better than the serial iterative scheme, which is in line with the previous prediction in Section 2.

Therefore, the parallel iterative version of multiplane GAA method was chosen to design the multiple phase distributions for phased array M3-DS. In order to theoretically investigate the prediction and this method, simulations were conducted. Assume that there are three scanning beams at a moment, each focal spot of the beams' are located at different spatial positions and especially located at different planes axially (e.g. Spot 1 in Plane 1, Spot 2 in Plane 2, Spot 3 in Plane 3), as shown in Fig. 4, and $\Delta z_1 = -5$ mm, $\Delta z_2 = 5$ mm, $\Delta z_3 = 11$ mm. Obviously, the three light spots projected onto the focal plane of the lens can be shown as the distribution in the dashed box (i.e. the “three fatter spots”). Because the absolute value of Δz_3 is maximum and the absolute values of Δz_1 and Δz_2 are equal. Thus, the intensity distribution of the middle one (i.e. the projection of the Spot 3) of the “three fatter spots” should be the largest while the other two should be the same, which was used to evaluate the effectiveness of the parallel iterative version of multiplane GAA method for phased array M3-DS.

In order to achieve the spatial positions of the three scanning beams detailed in Fig. 4, by using the parallel iterative version of multiplane GAA method, phase distributions were designed as displayed in Fig. 5, $\varphi_n^1(x, y), \varphi_n^2(x, y)$ and $\varphi_n^3(x, y)$ were respectively the designed phase distribution for the Spot 1, 2, and 3, $\varphi_F(x, y) = \varphi_n^1(x, y) + \varphi_n^2(x, y) + \varphi_n^3(x, y)$ was the final phase distribution which was to be loaded onto the phased arrays for the desired spatial positions of the Spot 1, 2, and 3 in Fig. 4.

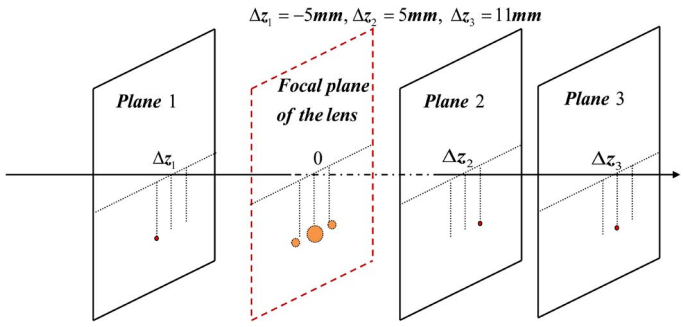

Fig. 4. Three light spots located at different spatial positions and their projection on the focal plane of the lens.

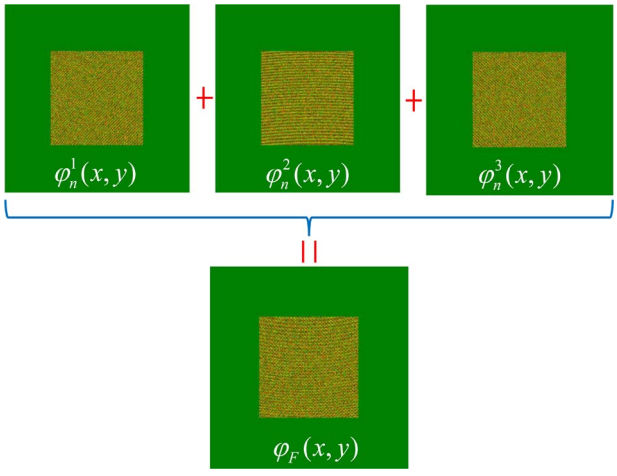

Fig. 5. Designed phase distributions for achieving the spatial positions of the three scanning beams detailed in Fig. 4.

The diffraction in the focal plane of the lens of this final phase distribution $\varphi_F(x, y)$ is shown in Fig. 6, four diffraction spots were obtained and the brightest one was the unwanted zero order of diffraction caused by the unmodulated part of the $\varphi_F(x, y)$. The plane view and the three-dimensional view of the diffraction result are respectively given in Fig. 6(a) and (b). As can be seen from Fig. 6(a) and (b), the intensity distribution of the middle one of the three diffraction spots is obviously largest, and the other two are nearly the same, which is agreed well with the above predictions, that the intensity distribution of the middle one (i.e. the projection of the Spot 3) of the three spots should be the largest due to the absolute value of Δz_3 is maximum, and the other two should be the same due to the absolute values of Δz_1 and Δz_2 are equal. Therefore, theoretically, a conclusion can be given that the parallel iterative version of multiplane GAA method can be applied to design phase distributions for the spatial scanning position of the Spot 1, 2, and 3 (shown in Fig. 4).

4. Experiments and Discussions

In this Section, experiments were conducted to investigate the parallel iterative version of multiplane GAA method for phased array M3-DS. As we all known, the commercial phase-only liquid crystal spatial light modulator (PO-LCSLM) is one kind of phased arrays [2]. In addition, the manufacturing technologies of the PO-LCSLM are relatively mature, and the major manufacturers are the Boulder Nonlinear Systems (BNS), Holoeye Corporation, Hamamatsu Corporation and so on. Here, a PO-LCSLM (P512-0635-DVI), had been bought from BNS, was adopted. The PO-LCSLM has an active area of approximately 7.68×7.68 mm^2 consisting of 512×512 pixels

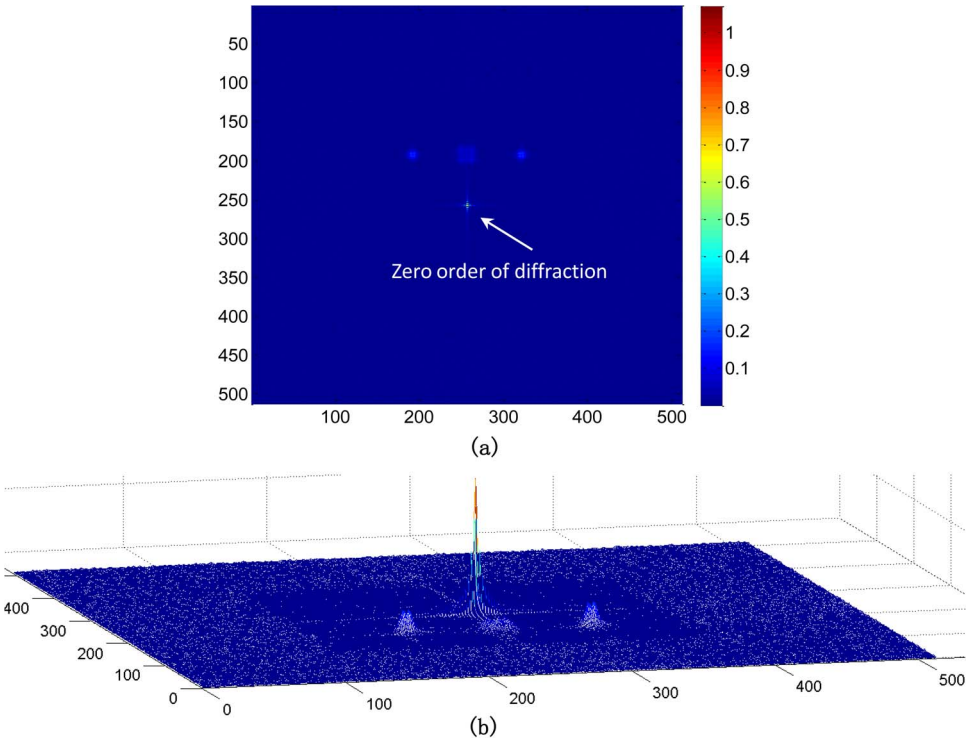

Fig. 6. Simulation of the diffraction of the phase distribution $\varphi_F(x, y)$ in the focal plane of the lens is obtained. (a) The plane view and (b) the 3-D view of the diffraction result.

(each pixel measures 15×15 μm^2; 1600 linear levels for 2π phase stroke; reflected wavefront distortion $\lambda/7$ and zero-order diffraction efficiency 61.5%). The CCD (GRAS-20S4M-C), supplied by Point Grey Corporation, has 1624×1224 pixels (each pixel measures 4.4×4.4 μm^2) and a 14 bit Analog-to-Digital Converter. Our experimental setup is detailed in Fig. 7. The phase distribution designed using the parallel iterative version of multiplane GAA method for M3-DS is loaded onto the PO-LCSLM and then it can retard the incident wavefront as the phase distribution does. According to the manual of the PO-LCSLM (P512-0635-DVI), the desired polarization alignment can be obtained by gradually rotating the passive half waveplate to achieve that the LCSLM to be in phase-only modulation mode (i.e. get the weakest zero order of diffraction). A passive half waveplate is used to facilitate achieving the desired polarization alignment, which guarantees the LCSLM to be in phase-only modulation mode (It should be noted that only a PO-LCSLM can be considered as the candidate of the phased arrays), and an variable optical attenuator is placed behind it for adjusting the intensity of the incident light. A 7.6 mm-expanded Gaussian beam from a HeNe laser ($\lambda = 632.8$ nm) incidents on to the PO-LCSLM. With a $f = 50$ mm Fourier lens, the diffraction in the focal plane of the Fourier lens are imaged by a CCD camera.

The phase distribution $\varphi_F(x, y)$ shown in Fig. 5, designed for the spatial scanning position of the Spot 1, 2, and 3 (shown in Fig. 4), was loaded onto the PO-LCSLM of this experimental setup. Then, the diffraction pattern measured by the CCD camera is shown in Fig. 8. The plane view and the 3-D view of the diffraction pattern are respectively given in Fig. 8(a) and (b). In the measured diffraction pattern, there are four diffraction spots and the brightest one is the unwanted zero order of diffraction caused by the unmodulated part of the PO-LCSLM displaying the $\varphi_F(x, y)$. As can be seen from Fig. 8(b), the intensity of the unwanted zero order of diffraction is saturated, however, the other three diffraction spots wanted is not saturated. Thus, the measured diffraction pattern is reliable and useable. As can be seen from Fig. 8(a) and (b), the intensity distribution of the middle one of the three diffraction spots is obviously largest, and the other two are nearly the same, which is agreed well with the simulation result in Fig. 6. So, it

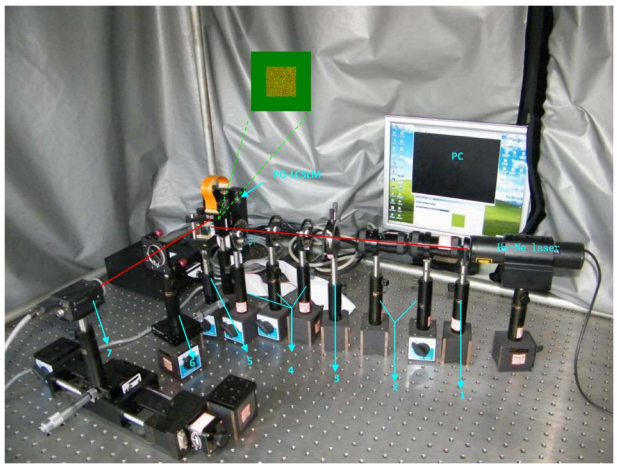

Fig. 7. Experimental setup. 1- aperture, 2- zoom beam expender, 3- passive half waveplate, 4- variable optical attenuator, 5- beam splitter, 6-Fourier lens, 7-CCD.

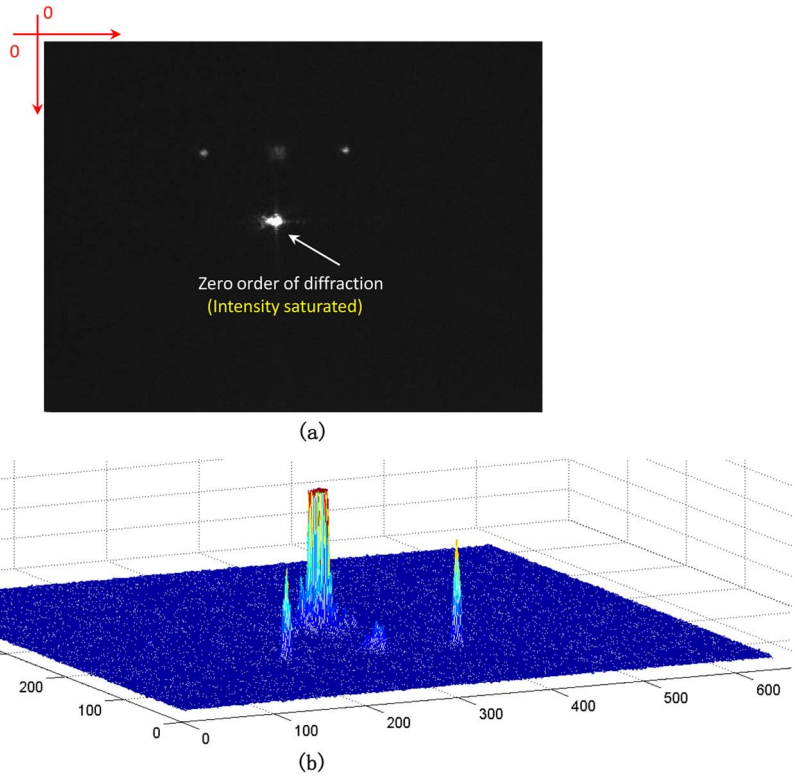

Fig. 8. Diffraction pattern is measured by the CCD camera when the phase distribution $\varphi_F(x, y)$ is loaded onto the PO-LCSLM. (a) The plane view and (b) the 3-D view of the measured diffraction pattern.

can be experimentally concluded that the parallel iterative version of multiplane GAA method can be applied to design phase distributions for the spatial scanning position of the Spot 1, 2, and 3 (shown in Fig. 4).

To further verify the practical feasibility of the parallel iterative version of multiplane GAA method for dynamic multi-beam 3-D scanning of the phased arrays, an additional experiment was conducted. Fig. 9 was given to demonstrate the lateral scanning and the axial scanning of

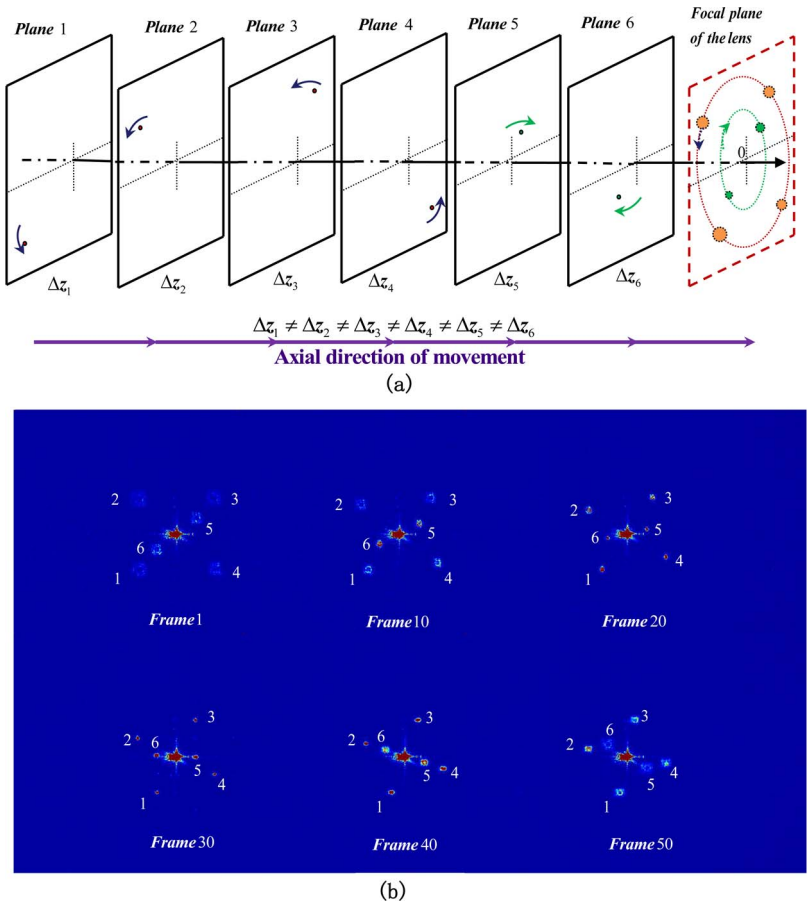

Fig. 9. Experimental results of the parallel iterative version of multiplane GAA method for dynamic multi-beam 3-D scanning of phased arrays.

the each spot of the randomly chosen multiple spots. As shown in Fig. 9(a), we randomly chose six spots which were set to be in six different planes and move along z-axis with a step of 500 um, meanwhile, the four spots of them (in planes 1, 2, 3, and 4) were expected to clockwise rotate around z-axis in each plane with a step of 12 um, the other two were expected to counterclockwise rotate around z-axis in each plane with a step of 12 um. Fifty phase distributions designed for scanning the six spots in fifty different positions were gradually loaded onto the phased array. Then, a dynamic sequence of diffraction patterns was measured by the CCD camera as shown in the GIF animation files (http://blog.sciencenet.cn/home.php?mod=space&uid=734814&do=blog&quickforward=1&id=820769), and the 1th, 10th, 20th, 30th, 40th, and 50th frame of the sequence are shown in Fig. 9(b). It can be found from the frames in Fig. 9(b) that spots 1, 2, 3, and 4 are controlled to clockwise rotate around z-axis and spots 5 and 6 are controlled to counterclockwise rotate around z-axis and this indicates that the lateral scanning of the randomly chosen six spots can be achieved. Meanwhile, as can be noted from the frame 1, 10, and 20 in Fig. 9(b) that each spot (e.g., spot 1) gradually becomes clear from blurred, and then gradually becomes blurred from clear as can be seen from the frame 30, 40, and 50 in Fig. 9(b), this is because that each spot (e.g., spot 1) is controlled to get in-focus and out-of-focus as the axial plane moves. The more detailed and dynamic demonstrations of the three dimensional scanning are given in the GIF animation files. And it can be seen from the GIF animation files and Fig. 9(b) that the three dimensional scanning of the six focal spots are realized as expected, which suggests the parallel iterative version of multiplane GAA method can be applied to design phase distributions for dynamic multi-beam 3-D scanning of the

phased arrays. This technique would provide a promising convenient multi-beam generating and 3-D scanning for ladar, laser weapons, laser micromachining, etc.

5. Conclusion

The most frequently used methods for the M2-DS of the phased arrays are the GS and GAA method. Recently, the GAA method had been proven to be better than GS method on the uniformity of the beam, while the efficiency of the light beam were almost the same for both of them [25], [26]. Since the GAA method is only suitable for creating phase distributions for phased arrays multi-beam independently lateral scanning, therefore, we propose the multiplane GAA method and firstly demonstrate it for phased arrays multi-beam independently generating and 3-D scanning. the multiplane GAA method is improved from the GAA method, but, a striking difference is that the iteration plane is not just one but multiple, which promises the method to be, not only capable of creating phase distributions for the independently axial scanning, but also suitable for creating phase distributions for phased array multi-beam independently lateral scanning.

Details of the mathematical expressions and two versions of the method are given to show the phase distributions design process for M3-DS. The parallel iterative version of multiplane GAA method has been numerically proven to be preferred for designing the multiple phase distributions for phased array M3-DS, and a simulation of the preferred method designing the multiple phase distributions for phased array M3-DS is conducted. Then, a corresponding experimental demonstration is investigated by using an optical setup based on a kind of phased arrays (PO-LCSLM), onto which the designed phase distributions are loaded. Simulation results agree well with experimental results, which validates the effectiveness of the method proposed. Finally, an additional experiment is conducted to further verify the practical feasibility of the proposed method for dynamic multi-beam 3-D scanning of phased arrays, and the results confirm the capabilities and practicalities of it. It can therefore be concluded that the method would provide a promising convenient multi-beam generating and 3-D scanning for ladar, laser weapons, laser micromachining, etc.

Acknowledgement

We thank the Editors/Reviewers for their constructive and helpful comments and suggestions for the paper.

References

[1] P. F. McManamon *et al.*, "Optical phased array technology," *Proc. IEEE*, vol. 84, no. 2, pp. 268–298, Feb.1996.
[2] P. F. McManamon *et al.*, "A review of phased array steering for narrow-band electrooptical systems," *Proc. IEEE*, vol. 97, no. 6, pp. 1078–1096, Jun. 2009.
[3] L. Xu, J. Zhang, and L. Y. Wu, "Influence of phase delay profile on diffraction efficiency of liquid crystal optical phased array," *Opt. Laser Technol.*, vol. 41, no. 4, pp. 509–516, Jun. 2009.
[4] N. A. Riza, "A compact high-performance optical control system for phased array radars," *IEEE Photon. Technol. Lett.*, vol. 4, no. 9, pp. 1072–1075, Sep. 1992.
[5] J. Sun, E. Timurdogan, A. Yaacobi, E. S. Hosseini, and M. R. Watts, "Large-scale nanophotonic phased array," *Nature*, vol. 493, no. 7431, pp. 195–199, Jan. 2013.
[6] T. A. Dorschner and W. M. Lipchak, "Laser radar system with phased-array beam steerer," U.S. Patent 5 253 033 A, Oct. 12, 1993.
[7] X. Wang, Q. Li, and Q. Wang, "Progress and analysis of the liquid crystal phased array technology in ladar," in *Proc. 10th RCSLPLT ASOT*, 2010, pp. 273–276.
[8] R. Aprahamian *et al.*, "Phased array combination of laser beams," U.S. Patent 4 794 345 A, Dec. 27, 1988.
[9] R. J. Beck *et al.*, "Application of cooled spatial light modulator for high power nanosecond laser micromachining," *Opt. Exp.*, vol. 18, no. 16, pp. 17059–17065, 2010.
[10] N. J. Jenness *et al.*, "Three-dimensional parallel holographic micropatterning using a spatial light modulator," *Opt. Exp.*, vol. 16, no. 20, pp. 15942–15948, Sep. 2008.
[11] X. Wang, D. Wilson, R. Muller, P. Maker, and D. Psaltis, "Liquid-crystal blazed-grating beam deflector," *Appl. Opt.*, vol. 39, no. 35, pp. 6545–6555, Dec. 2000.
[12] X. Liu, J. Zhang, L. Y. Wu, and Y. Gan, "Fast generation of controllable equal-intensity four beams based on isosceles triangle multilevel phase grating realized by liquid crystal spatial light modulator," *Chin. Phys. B*, vol. 20, no. 2, pp. 024211-1–024211-8, Feb. 2011.

[13] X. Lin, H. Zi-Qiang, and Y. Ruo-Fu, "Programmable agile beam steering based on a liquid crystal prism," *Chin. Phys. B*, vol. 20, no. 11, pp. 114216-1–114216-6, 2011.
[14] X. Tan, B. Gu, and G. Yang, "Diffractive phase elements for beam shaping: A new design method," *Appl. Opt.*, vol. 34, no. 8, pp. 1314–1320, Mar. 1994.
[15] G. Zhang, B. Gu, and G. Yang, "Design of diffractive phase elements that produce focal annuli a new method," *Appl. Opt.*, vol. 34, no. 35, pp. 8110–8115, Dec. 1995.
[16] R. W. Gerchberg and W. O. Saxton, "Phase determination from image and diffraction plane pictures in electron microscope," *Optik*, vol. 34, 237–246 (1971).
[17] R. W. Gerchberg and W. O. Saxton, "A practical algorithm for determination of phase from image and diffraction plane pictures," *Optik*, vol. 35, pp. 275–284, 1972.
[18] J. E. Curtis, B. A. Koss, and D. G. Grier, "Dynamic holographic optical tweezers," *Opt. Commun.*, vol. 207, no. 1–6, pp. 169–175, 2002.
[19] R. Di Leonardo, F. Ianni, and G. Ruocco, "Computer generation of optimal holograms for optical trap arrays," *Opt. Exp.*, vol. 15, no. 4, pp. 1913–1922, Feb. 2007.
[20] J. Liesener, M. Reicherter, T. Haist, and H. J. Tiziani, "Multi-functional optical tweezers using computer-generated holograms," *Opt. Commun.*, vol. 185, no. 1–3, pp. 77–82, Nov. 2000.
[21] T. Haist, M. Schonleber, and H. J. Tiziani, "Computer-generated holograms from 3D-objects written on twisted-nematic liquid crystal displays," *Opt. Commun.*, vol. 140, no. 4–6, pp. 299–308, Aug. 1997.
[22] G. Sinclair *et al.*, "Interactive application in holographic optical tweezers of a multi-plane Gerchberg–Saxton algorithm for three-dimensional light shaping," *Opt. Exp.*, vol. 12, no. 8, pp. 1665–1670, Apr. 2004.
[23] G. Shabtay, "Three-dimensional beam forming and Ewald's surfaces," *Opt. Commun.*, vol. 226, no. 1–6, pp. 33–37, Oct. 2003.
[24] G. Whyte and J. Courtial, "Experimental demonstration of holographic three-dimensional light shaping using a Gerchberg–Saxton algorithm," *New J. Phys.*, vol. 7, no. 1, pp. 117, May 2005.
[25] M. Pasienski and B. DeMarco, "A high-accuracy algorithm for designing arbitrary holographic atom traps," *Opt. Exp.*, vol. 16, no. 3, pp. 2176–2190, Feb. 2008.
[26] D. Wang, J. Zhang, H. Wang, and Y. Xia, "Variable shape or variable diameter flattop beam tailored by using an adaptive weight FFT-based iterative algorithm and a phase-only liquid crystal spatial light modulator," *Opt. Commun.* vol. 285, no. 24, pp. 5044–5050, Nov. 2012.